DEVELOPMENTAL BIOLOGY

# Deficiency of TRPM2 leads to embryonic neurogenesis defects in hyperthermia

Yanxin Li[1,2] and Jianwei Jiao[1,2,3,4]*



**Temperature homeostasis is critical for fetal development. The heat sensor protein TRPM2 (transient receptor potential channel M2) plays crucial roles in the heat response, but its function and specific mechanism in brain development remain largely unclear. Here, we observe that TRPM2 is expressed in neural stem cells. In hyperthermia, *TRPM2* knockdown and knockout reduce the proliferation of neural progenitor cells (NPCs) and, accordingly, increase premature cortical neuron differentiation. In terms of the mechanism, TRPM2 regulates neural progenitor self-renewal by targeting SP5 (specificity protein 5) via inhibiting the phosphorylation of β-catenin and increasing β-catenin expression. Furthermore, the constitutive expression of TRPM2 or SP5 partly rescues defective NPC proliferation in the TRPM2-deficient embryonic brain. Together, the data suggest that TRPM2 has a critical function in maintaining the NPC pool during heat stress, and the findings provide a framework for understanding how the disruption of the *TRPM2* gene may contribute to neurological disorders.**

## INTRODUCTION

The cerebral cortex is the most evolved and complicated structure in the mammalian brain and has many physiological functions, such as attention, cognition, learning, and memory. The functions rely on the detailed cortex structure, which includes a six-layered architecture formed by migrating neurons in an inside-out pattern (*1*). These plentiful neurons are generated from various neural progenitor cells (NPCs). The primary progenitor cells are radial glial (RG) cells, which are mainly responsible for self-renewal and result in the expansion of the cortex, the differentiation of neurons, and the production of postmitotic neurons (*2*). The process of neuronal production, also known as neurogenesis, plays crucial roles in cerebral development and can affect the function of the neocortex. Generally, each process in neurogenesis, including self-renewal, differentiation, and the maturation of neurons, is strictly regulated, and any disturbance leads to severe disorders (*3*). The entire process is regulated by numerous extracellular and intracellular signals and factors. Any stress or unusual stimulus may lead to abnormalities in brain function.

During pregnancy, various stimuli can lead to abnormal neural development (*4*, *5*). Among them, heat stress is an important stimulus for both the mother and fetus during pregnancy, and maternal thermal homeostasis is critical for fetal survival and ontogenesis. For example, maternal fever during the gestation period is associated with congenital heart defects and neural tube defects (*6*, *7*). However, it is largely unknown whether heat stress, such as hyperthermia, disturbs neurogenesis and cortical development.

A series of thermally activated ion channels has been reported to detect the entire thermal range (*8*, *9*). Among them, transient receptor potential channel M2 (TRPM2) is a plasma membrane calcium-permeable cation channel and is a unique member of the TRP family that is sensitive to various signals. Recently, studies have reported that TRPM2 can be activated by heat and that the deletion of TRPM2 in mice results in a remarkable deficit in their perception of nonpainful warm stimuli in the range of 33° to 38°C (*10*). TRPM2 has been implicated in several neurodevelopmental/neurological disorders including bipolar disorder, neuropathic pain, and Parkinson's disease (*11*). In addition, TRPM2 has been shown to participate in various biological processes, including insulin secretion, $H_2O_2$-induced cell apoptosis, and brain damage following ischemic insults in adult and neonatal mice (*12*–*14*). Therefore, it is crucial to investigate the precise functions and molecular mechanisms of the hyperthermia-related protein TRPM2 and characterize the protein's role in the regulation of brain development during heat stress and maternal hyperthermia.

Several pieces of evidence have demonstrated that canonical Wnt signaling, including β-catenin, which acts as a core downstream effector, determines the transition from neuronal proliferation to differentiation during cortical neurogenesis. In the early stages of neurogenesis, the overexpression of β-catenin in NPCs promotes their proliferation, whereas a deficiency in β-catenin in NPCs facilitates neurogenesis (*15*). The precise signal transductions that modulate neurogenesis are unclear and need further elucidation. The transcription factor SP5 (specificity protein 5) is a member of the SP transcription factor family (*16*), and previous studies have shown that SP5 plays a crucial role in governing mouse embryonic stem cell pluripotency (*17*) and neural crest specification (*18*). During vertebrate development, SP5 acts downstream of Wnt/β-catenin signaling in neuroectoderm patterning (*19*). In addition, the hypermethylation of SP5 has been implicated in schizophrenia, a neuropsychiatric disorder associated with the dysregulation of neural stem cell (NSC) proliferation and differentiation (*20*, *21*). However, the role of SP5 in hyperthermia during neurogenesis has never been reported.

Here, we demonstrate that the thermo-sensor protein TRPM2 is enriched in the embryonic cerebral cortex and that its expression gradually increases during heat stress. We also show that TRPM2-deficient mice exposed to heat show reduced NSC proliferation and a premature shift in RG differentiation. Mechanistically, this study identifies an important role of TRPM2 in modulating SP5 expression by inhibiting the phosphorylation of β-catenin in sustaining neural progenitor self-renewal during heat stress. In addition, the heat-induced proliferation defects caused by TRPM2 knockdown or

[1]State Key Laboratory of Stem Cell and Reproductive Biology, Institute of Zoology, Chinese Academy of Sciences, Beijing 100101, China. [2]University of Chinese Academy of Sciences, Beijing 100049, China. [3]Co-Innovation Center of Neuroregeneration, Nantong University, Nantong 226001, China. [4]Institute for Stem Cell and Regeneration, Chinese Academy of Sciences, Beijing 100101, China.
*Corresponding author. Email: jwjiao@ioz.ac.cn

knockout can be partially rescued by the overexpression of SP5. Collectively, these findings reveal that the heat sensor protein TRPM2 has a previously unidentified role in modulating cortical neurogenesis during hyperthermia conditions. These findings provide previously unknown insights to further elucidate neurological disorders associated with heat stress and reveal previously unidentified strategies for treatment.

## RESULTS

### Thermal stimuli affect NSC proliferation and cell positioning

To determine the effect of heat stress on the developing cortex, we performed stress experiments in which pregnant mice were placed in a thermostatic biochemical incubator (fig. S1A) set to 38°C for 2 hours from embryonic day 13.5 (E13.5) to E15.5; the control group was kept at room temperature. After heat stress, E15.5 brain slices were stained with an antibody against mitotic index PH3. Compared with that in the control group, the number of PH3-positive cells residing at both the apical and basal positions was notably augmented, indicating that heat stress promoted mitotic activity (Fig. 1, A to C). Consistently, double staining for bromodeoxyuridine (BrdU) with PAX6 (one type of neural progenitor marker) (Fig. 1, D and E) and TBR2 (an intermediate progenitor marker) (Fig. 1, F and G) revealed that the number of cells in the proliferative state was increased in hyperthermia. Collectively, these results indicate that heat stress promotes neural progenitor self-renewal. In a second group of pregnant mice, similar heat stress was induced at E13.5 to E16.5; then, in utero electroporation (IUE) was performed to analyze embryonic brain development. When embryos were electroporated with a green fluorescent protein (GFP)–encoding plasmid, which was used as a control plasmid on E13.5 and collected on E16.5, the hyperthermia group showed an abnormal distribution, which manifested as an increase in the number of cells in the ventricular zone/subventricular zone (VZ/SVZ) and a reduction in the number of GFP-positive cells in the cortical plate (CP) compared with those in the room temperature group (Fig. 1, H and I). In our research, the control mice were maintained in the vivarium at room temperature. We also conducted IUE experiments when mice were maintained in an incubator or in the vivarium at room temperature and found that the stress experienced by the mother due to moving to a new environment did not play a role in the observed phenotypes (fig. S1, B and C). Together, these results demonstrate that heat stress may disturb neurogenesis during embryonic brain development.

### The heat sensor protein TRPM2 is expressed in neural progenitors during embryonic brain development

It has been reported that many receptors are thermally sensitive (*10*). To verify heat sensitivity, we housed pregnant mice with E13.5 fetuses at 38°C for 2 hours for 3 days. Control pregnant mice were kept at room temperature. After 3 days (i.e., E15.5), RNA was extracted from the cerebral tissues of fetal mice. We detected the RNA levels of several receptors associated with heat (*10*, *22*) and observed that in mice subjected to heat stress, the mRNA levels of only *TRPM2*, among the numbers of the TRP family, increased significantly (Fig. 1J). Molecular markers of heat-sensitive neurons within the preoptic hypothalamus were also affected. *BDNF* and *PACAP* mRNA levels increased (fig. S1D), which is consistent with previous studies (*23*). To examine the specific expression pattern of TRPM2 in the early embryonic brain, we conducted immunofluorescence and colocalization analyses. In vivo, the brain sections of E13.5 and E15.5 mice were collected and stained with antibodies against TRPM2 and the two neural progenitor markers, namely, NESTIN (*24*) and SOX2 (sex-determining region Y–related HMG box 2). TRPM2 was observed to be colocalized with NESTIN-positive and SOX2-positive progenitor cells and resided in the VZ/SVZ of the cerebral cortex in both E13.5 and E15.5 brain sections from mice housed at room temperature (Fig. 1K and fig. S1E). In addition, in vitro, we observed that TRPM2 was coexpressed with NESTIN and SOX2 in primary mouse NSCs derived from E12.5 cerebral tissues and cultured in proliferation medium for 2 days (Fig. 1L). Next, to investigate TRPM2 expression at different developmental stages, we harvested cerebral tissues from E13.5, E15.5, and E18.5 and analyzed them using Western blotting. The results revealed that TRPM2 expression gradually increased from E13.5 to E18.5 (fig. S1, F and G). We also investigated TRPM2 transcription in vivo using cortical tissues and in vitro using NPCs cultured under differential or proliferative conditions. Reverse transcription polymerase chain reaction (RT-PCR) was performed on RNA extracted from the tissues or the NPCs. All data indicated that the mRNA levels of TRPM2 showed an obvious up-regulation as embryonic development proceeded (fig. S1, H to J). In addition, another group of pregnant mice was housed at 38°C for 2 hours for 3 days at E15.5. Heat-treated mice showed a marked augmentation of TRPM2 expression in the VZ/SVZ of the neocortex compared with that in control mice (Fig. 1, M and N). Overall, these findings suggest that TRPM2, especially during heat stress, plays an important role in modulating NSC neurogenesis during embryonic cortical development.

### *TRPM2* knockdown leads to abnormal cell distribution during heat stress

On the basis of the distinctive expression pattern of TRPM2 in NSCs, we explored whether TRPM2 plays a unique role in neurogenesis during embryonic brain development. We generated a *TRPM2*-targeting short hairpin RNA (shRNA) plasmid and a *TRPM2*-overexpressing lentiviral-based vector to effectively silence and augment TRPM2 expression, respectively, in neural progenitors. In NPCs (Fig. 2, A and B, and fig. S1M), N2A cells (fig. S1, L and O), and 293FT cells (fig. S1N) treated with our constructs, Western blotting confirmed TRPM2 knockdown or overexpression. To verify our strategy, we further confirmed *TRPM2* shRNA knockdown efficiency by real-time PCR analysis in NSCs, and the analysis showed that TRPM2 levels were effectively suppressed (fig. S1K). Next, we investigated whether TRPM2 disturbs cell distribution in vivo using IUE. In E13.5 mice, brains were injected and electroporated with the *TRPM2* shRNA or control plasmid, and the mice were sacrificed at E16.5 for phenotypic analysis. We observed no obvious change in the distribution of GFP-positive cells across the cerebral cortex (fig. S2, A and B). However, the more interesting observation was that when maternal mice were placed in a 38°C temperature-controlled incubator for 2 hours from E14.5 to E16.5, *TRPM2* knockdown resulted in an obvious reduction in the number of GFP-positive cells in the VZ/SVZ and a corresponding increase in the number of GFP-positive cells in the CP (Fig. 2, C and D). When a 39°C temperature-controlled incubator was used, similar results were obtained (fig. S2, C and D). To observe more long-term effects, we performed IUE at E13.5 to E17.5 and comparable GFP-positive cell distributions were observed (fig. S2, E and F). In addition, we also sought to determine whether the knockdown of

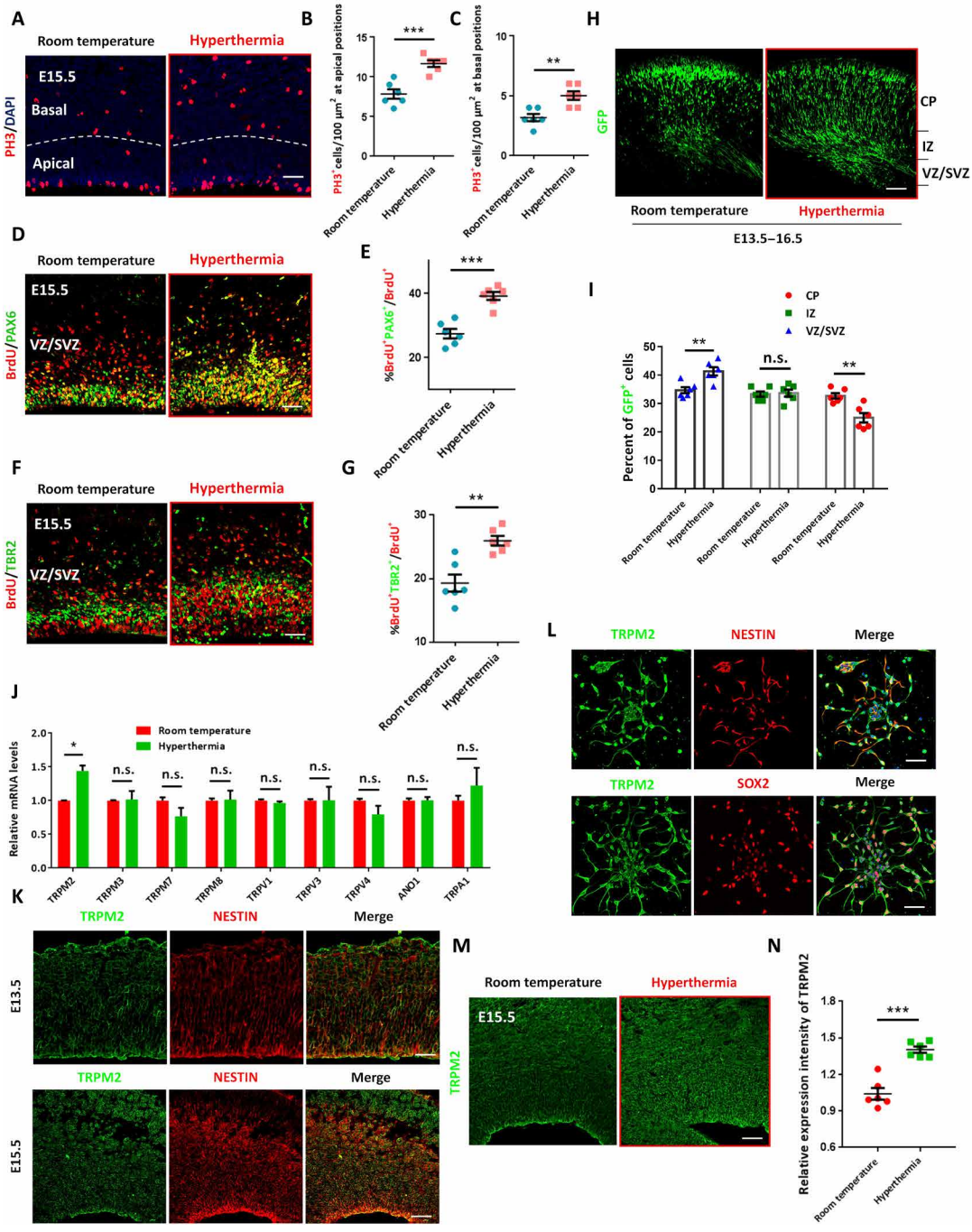


**Fig. 1. Heat stress affects embryonic brain development.** (**A** to **C**) E15.5 brain sections from the room temperature and hyperthermia groups were immunolabeled with the mitotic marker PH3 and 4′,6-diamidino-2-phenylindole (DAPI). The graphs show the number of $PH3^+$cells per 100 $\mu m^2$ at the apical and basal positions ($n = 6$). Scale bar, 20 μm. (**D** to **G**) Mice underwent 2 hours of BrdU pulse labeling and were euthanized at E15.5. Brain slices were then double stained with antibodies against BrdU/PAX6 and BrdU/TBR2. The graphs show the populations of $BrdU^+PAX6^+$ and $BrdU^+TBR2^+$ cells relative to the total population of $BrdU^+$ cells ($n = 6$). Scale bars, 20 μm. (**H** and **I**) Thermal stimuli lead to the abnormal distribution of GFP-positive cells in the developing neocortex. An electroporation experiment was conducted at E13.5, and embryonic brains were collected on E16.5. The percentage of GFP-positive cells in each region is displayed in the bar graph ($n = 6$ embryos from four different mothers). Scale bar, 50 μm. IZ, intermediate zone. (**J**) Reverse transcription polymerase chain reaction (RT-PCR) results showing the relative mRNA levels of members of the TRP family in the heat stress experiment ($n = 3$). n.s., not significant. (**K**) TRPM2 is abundantly enriched in NESTIN-positive NSCs in the embryonic cerebral cortex. E13.5 and E15.5 brain slices were immunostained with anti-NESTIN and anti-TRPM2 antibodies (VZ/SVZ) ($n = 5$). Scale bars, 20 μm. (**L**) TRPM2 is expressed and colocalized with SOX2 and NESTIN in primary NSCs. The cells were collected from the cerebral cortex of E12.5 mouse brains and maintained in proliferative medium for 24 hours ($n = 4$). Scale bars, 20 μm. (**M** and **N**) TRPM2 expression increases at warm temperatures in the E15.5 cerebral cortex. E15.5 brain sections were stained with an antibody against TRPM2. The graph shows the relative expression intensities of TRPM2 ($n = 6$). The intensity of TRPM2 was quantified with ImageJ. Scale bar, 20 μm. The data are shown as means ± SEM; two-tailed Student's *t* tests; $^*P < 0.05$, $^{**}P < 0.01$, and $^{***}P < 0.001$ versus the indicated group.

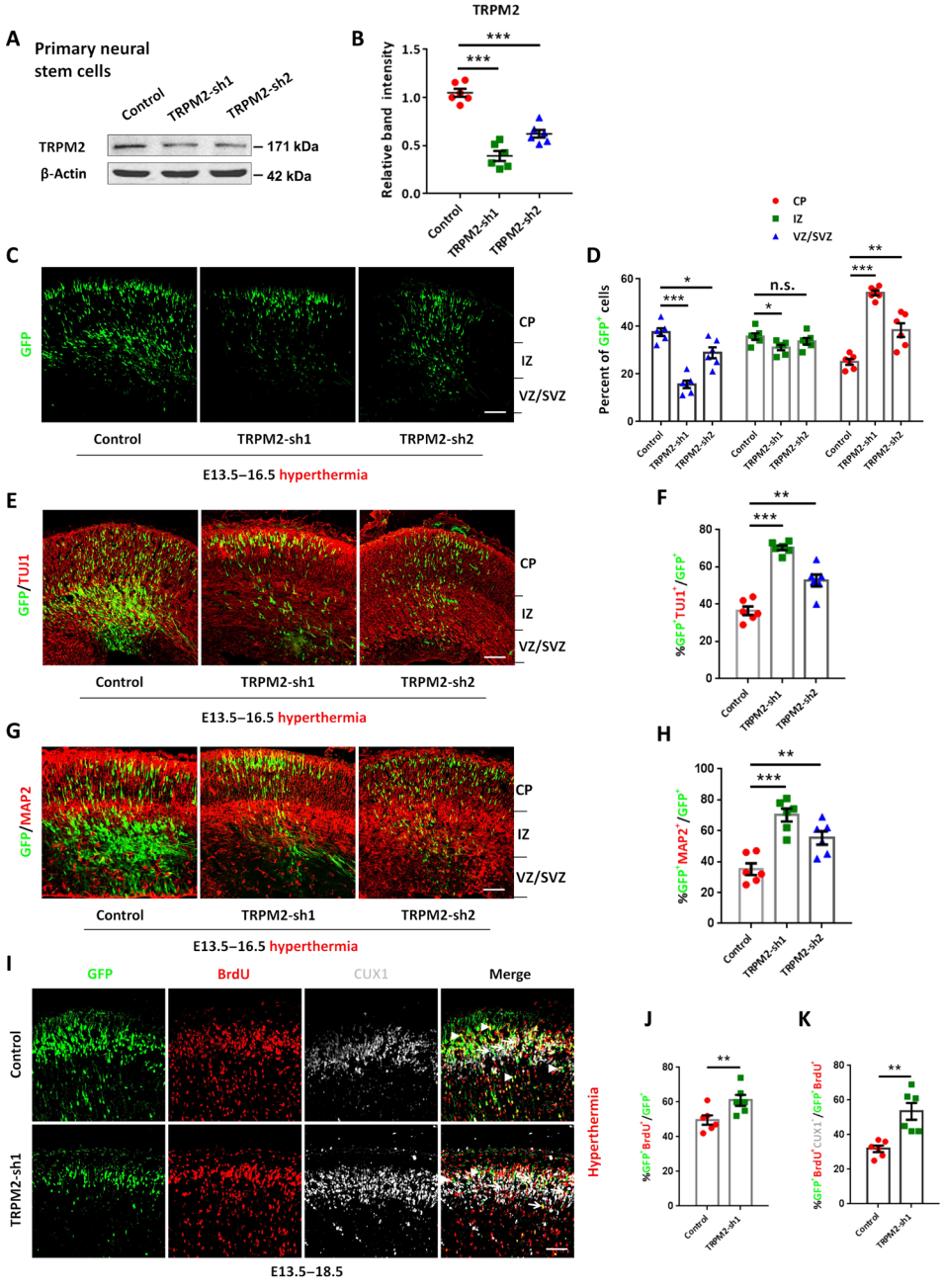


**Fig. 2. *TRPM2* knockdown leads to abnormal cell distribution and the enhanced differentiation of NSCs during heat stress.** (**A**) Western blot analysis confirmed the knockdown (empty pSicoR shRNA was used as a control) of *TRPM2* in cultured NSCs. β-Actin was used as a control. (**B**) The graph shows that TRPM2 expression levels were effectively knocked down in primary NSCs by *TRPM2*-shRNA ($n = 6$). (**C** and **D**) *TRPM2* knockdown alters the distribution of cells in the cerebral cortex during heat stress. A control or *TRPM2* shRNA plasmids were microinjected and electroporated into the brains of E13.5 mice, and brains were collected on E16.5. During the process, the mice were exposed to 38°C for 2 hours per day from E14.5 to E16.5. The GFP-positive cell populations in each region are displayed in the bar graph ($n = 6$ embryos from four different mothers). Scale bar, 50 μm. (**E** and **F**) The number of $TUJ1^+GFP^+$ cells is augmented in *TRPM2* shRNA–treated animals subjected to heat stress. Brain slices from E16.5 mice were stained with an antibody against TUJ1. The population of $TUJ1^+GFP^+$ cells relative to the total population of $GFP^+$ cells is shown in the bar graph ($n = 6$ embryos from four different mothers). Scale bar, 50 μm. (**G** and **H**) The number of $MAP2^+GFP^+$ cells is slightly increased in *TRPM2* shRNA–treated animals in hyperthermia. E16.5 brain slices were stained with an anti-MAP2 antibody. The population of $MAP2^+GFP^+$ cells relative to the total population of $GFP^+$ cells is shown in the bar graph ($n = 6$ embryos from four different mothers). Scale bar, 50 μm. (**I**) Silencing *TRPM2* induces NPC terminal mitosis during heat stress. A *TRPM2* shRNA or control plasmid was injected and electroporated into E13.5 mouse brains. BrdU was gently injected 24 hours after electroporation at E14.5, and the electroporated brains of the embryos were collected for analysis at E18.5. Immunohistochemical analysis was performed using anti-BrdU and anti-CUX1 antibodies. During the process, the mice were exposed to 38°C for 2 hours per day from E14.5 to E18.5. The arrowheads represent $BrdU^+/GFP^+$ cells, and the arrows represent $GFP^+BrdU^+CUX1^+$ cells. Scale bar, 20 μm. (**J**) Bar graph displaying the population of $BrdU^+GFP^+$ cells relative to the total number of GFP-positive cells in the CP ($n = 6$ embryos from four different mothers). (**K**) Quantification of the population of $GFP^+BrdU^+CUX1^+$ cells relative to the population of $GFP^+BrdU^+$ cells ($n = 6$ embryos from four different mothers). The data are shown as means ± SEM; two-tailed Student's *t* tests; $^*P < 0.05$, $^{**}P < 0.01$, and $^{***}P < 0.001$ versus the indicated group.

*TRPM2* has a possible effect on cell migration. IUE experiments are frequently used to monitor cell migration during embryonic cerebral development (*25*–*27*). Then, we performed an E15.5-to-E19.5 IUE experiment in mice at room temperature and an E14.5-to-E18.5 IUE experiment in mice exposed to heat (fig. S2, G to I) and found that there was nearly no difference in GFP distribution from the VZ/SVZ to the CP between the control and *TRPM2* knockdown groups. These results jointly eliminated the influence of *TRPM2* depletion on cell migration. Thus, the data suggest that TRPM2 may take part in regulating neurogenesis during heat stress.

### *TRPM2* knockdown in hyperthermia prohibits NSC proliferation and facilitates cell cycle exit

On the basis of the reduction in the number of GFP-positive cells in the VZ/SVZ, which enriches NPCs, we considered the possibility that TRPM2 plays a vital role in modulating NSC proliferation in hyperthermia. To address this possibility, we injected BrdU into pregnant mice 2 hours before the collection of electroporated embryonic brains. In *TRPM2* knockdown mice, heat stress at E13.5 to E16.5 led to a marked reduction in the percentage of $GFP^+BrdU^+$ cells (fig. S3, A to C), the percentage of $GFP^+BrdU^+PAX6^+$ cells (fig. S3, D and E), the expression of mitotic marker PH3 (fig. S3, F and G), and the expression of TBR2 (fig. S3, H and I) in NPCs residing in the VZ/SVZ.

Together, these results indicate that TRPM2 is vital for maintaining the NSC pool. To further explore whether a decrease in NPC proliferation leads to precocious cortical neurogenesis, we analyzed cell cycle exit. After electroporating control or *TRPM2*-shRNA plasmids into embryonic brains at E13.5, BrdU was injected 24 hours before the collection of electroporated brains from embryos on E15.5 and from E14.5 to E16.5. During the process, the pregnant mice were kept at 38°C for 2 hours per day. Next, we stained brain slices with antibodies against BrdU and the proliferative marker KI67 to evaluate cells that precociously exit the cell cycle. We observed a substantial augmentation of the indicator of cell cycle exit in the *TRPM2*-silenced group that was subjected to heat stress, confirming that the elimination of *TRPM2* facilitated cell cycle exit in response to hyperthermia (fig. S4, A to C).

### Suppression of *TRPM2* accelerates neuronal differentiation and neural progenitor terminal mitosis during hyperthermia

To verify the possibility that *TRPM2* knockdown NPCs that exit the cell cycle during heat stress may differentiate prematurely into neurons, we stained brain sections with an antibody against TUJ1 (β-III-tubulin, a neuronal marker) to label neurons. Analysis revealed an obvious change in the percentage of $TUJ1^+/GFP^+$ cells in brain slices from *TRPM2* knockdown mice subjected to heat stress (Fig. 2, E and F). We also observed a remarkable increase in the number of cells expressing the neuronal or upper layer markers $MAP2^+/GFP^+$ (Fig. 2, G and H), $SATB2^+/GFP^+$ (fig. S4, D and E), and $CUX1^+/GFP^+$ (fig. S4, F and G) and a decrease in the number of cells expressing CTIP2 (a marker of deep layer neurons)$^+/GFP^+$ (fig. S4, I and J) compared to those in control brain slices, suggesting an increase in the differentiation of NSCs. We also birthdated neurons using BrdU to investigate whether *TRPM2* knockdown accelerates the terminal mitosis of premature neural progenitors in mice challenged with heat. As previously described (*28*), BrdU was injected into the abdominal cavity of pregnant mice 24 hours after the electroporation of E14.5 fetuses, and the electroporated brains of the embryos were collected for analyses at E18.5 (fig. S4H). Because BrdU labels dividing cells in the S phase (*29*), the label becomes diluted and gradually disappeared upon the self-renewal of NPCs. Only cells that differentiate into neurons within the CP layer during their final mitotic division are permanently labeled. By staining with an antibody against BrdU, we observed a marked increase in the number of $BrdU^+/GFP^+$ (Fig. 2, I and J) cells in the *TRPM2* shRNA–treated brains compared with control shRNA–treated brains. When colocalized with the outer cortical layer marker CUX1, a significant change in the percentage of $CUX1^+GFP^+BrdU^+$ cells relative to that of $GFP^+BrdU^+$ cells in the *TRPM2* shRNA–treated group was observed. These results indicate that more BrdU-labeled NPCs differentiated into CUX1-positive neurons in the CP in the *TRPM2* shRNA–treated group (Fig. 2K). Collectively, these findings effectively demonstrate that during heat stress, *TRPM2* loss of function results in augmented terminal mitosis and enhanced cortical neuronal differentiation.

### Depletion of *TRPM2* during heat stress affects the development and morphology of cultured neurons

To verify the role of TRPM2 in neuron development under conditions of heat, we conducted an in vitro experiment using cultured primary NSCs. NPCs obtained from the E12.5 cerebral cortex were infected with either a control or *TRPM2* shRNA plasmid–packaged lentivirus. After 24 hours, the cells were then incubated at 38°C for 3 days in proliferative medium and finally stained with antibodies against TUJ1 and KI67. We observed an obvious increase in the number of $GFP^+TUJ1^+$ cells (fig. S5, A and B) and a marked decrease in the number of $GFP^+KI67^+$ cells (fig. S5, C and D) in *TRPM2*-deficient cells compared with control cells, supporting our in vivo findings. However, when NPCs were incubated at 37°C for 3 days, we observed no obvious change in the percentage of $GFP^+TUJ1^+$ cells in the *TRPM2*-deficient cells (fig. S6, H and I).

To further investigate the effects of TRPM2 on NPC morphology during heat stress, we kept NSCs acquired from E12.5 brains in differentiation medium at 38°C for 3 days. Using confocal imaging, we observed that compared with control NSCs, TRPM2 knockdown NSCs exhibited longer neurite outgrowth and increased branching after hyperthermia (fig. S5, H to J).

In addition, IUE was performed at E13.5, and the GFP-positive region of the brains from the embryo was collected and digested 2 days after electroporation at E15.5. During E14.5 to E15.5, the pregnant mothers were held at 38°C for 2 hours per day. Embryonic GFP-positive brain cells were acquired using fluorescence-activated cell sorting and then cultured for 2 days in proliferative medium at 38°C. Notably, *TRPM2*-silenced cells obtained from embryos whose mothers were heat-challenged showed prominent branching and longer neurite outgrowth compared with empty vector–treated cells (fig. S5, E to G). Jointly, these results suggest that TRPM2 can inhibit neuronal development during heat stress and is required for maintaining stem cell self-renewal.

### TRPM2 overexpression promotes the proliferation of NPCs during heat stress

In E13.5 mice electroporated with a TRPM2 overexpression vector, we observed a prominent increase in the number of GFP-positive cells residing in the VZ/SVZ and a corresponding decrease in the number of GFP-positive cells in the CP at E16.5 when pregnant mothers were subjected to heat stress for 2 hours from E14.5 to E16.5 (fig. S6, A and B). Compared to the normal expression of

TRPM2, TRPM2 overexpression during heat stress also led to more BrdU-positive cells in the VZ/SVZ (fig. S6, C to E), supporting a role for TRPM2 in promoting NSC proliferation. In addition, TRPM2 overexpression was found to rescue abnormal NPC distribution caused by the depletion of *TRPM2* in vivo (fig. S6, F and G), demonstrating that TRPM2 is required for the proliferation of NPCs during heat stress.

### *TRPM2* deletion leads to abnormal neurogenesis during heat stress

To further explore the phenotype of *TRPM2* knockout mice, we generated mice using the CRISPR-Cas9 system through zygote microinjection. The coding sequence (CDS) of *TRPM2* is located in exon 3, but not exon 1. After CRISPR editing, a termination codon was introduced near the start codon in the CDS (Fig. 3A). Genotyping PCR (Fig. 3B), Western blotting (fig. S7A), and real-time PCR (fig. S7B) were all performed to identify the knockout efficiency at the genome, protein, and RNA levels, respectively. We verified the knockout of *TRPM2* in pregnant *TRPM2* knockout mice exposed to hyperthermia at E14.5 to E16.5 by immunostaining E16.5 brain slices with an antibody against TRPM2 (fig. S7C). In addition, by immunostaining with an antibody against cleaved caspase-3, we observed that, in hyperthermia, there was no significant difference in the number of cleaved caspase-3$^+$ cells per field between E16.5 *TRPM2*$^{+/+}$ and *TRPM2*$^{-/-}$ brain slices, suggesting that *TRPM2* knockout had no effect on cell apoptosis under conditions of heat (fig. S7, D and E).

Next, we obtained E16.5 *TRPM2*$^{+/+}$ or *TRPM2*$^{-/-}$ embryonic brains from mothers that had been housed at 38°C for 2 hours per day from E14.5 to E16.5. By staining analysis, we observed fewer neural progenitors expressing PH3 (Fig. 3, C and G) and BrdU/PAX6 (Fig. 3, D and H) in the VZ/SVZ and more neurons expressing CUX1 (Fig. 3, E and I) and SATB2 (Fig. 3, F and J) in the CP in *TRPM2* knockout brain slices. In addition, when immunostaining for TRPM2 together with NESTIN or TUJ1 was performed on E16.5, we found that the expression of NESTIN was decreased, while the level of TUJ1 was observably augmented after the deletion of *TRPM2* in hyperthermia (fig. S7, F and G). Consistently, when mice were housed at 38°C for 2 hours per day from E14.5 to E18.5, more neurons expressing CUX1 were observed in the CP in *TRPM2* knockout brain slices both on postnatal day 0 (P0) and P6 (fig. S8, F to I), which suggests that the heat-mediated shift in the proliferation to differentiation ratio upon *TRPM2* knockout has a consistent and longer-term effect in later stages of development. However, in brain slices obtained from embryos of mothers who had been housed at room temperature, we did not find an obvious difference in TUJ1 staining at P0 between the wild-type and *TRPM2* knockout groups (fig. S8J). Consistently, progenitors isolated from hyperthermic E12.5 *TRPM2*$^{-/-}$ embryos developed longer neurites and more branching after culture in differentiation medium for 3 days than those of hyperthermic E12.5 *TRPM2*$^{+/+}$embryos, while room temperature embryos lacked these phenotypes (fig. S8, A to E). These observations suggest that *TRPM2* knockout and hyperthermia accelerate neuron development. In addition, NSCs obtained from E12.5 *TRPM2*$^{-/-}$ embryos formed smaller neurospheres than those of controls in hyperthermia, but not room temperature conditions, suggesting that the loss of *TRPM2* inhibits NPC proliferation during hyperthermia (fig. S7, K to M). To validate the function of TRPM2 during cortical neurogenesis in times of hyperthermia, we electroporated the brains of fetal *TRPM2*$^{+/+}$ and *TRPM2* $^{-/-}$ mice with control plasmids and brains of fetal *TRPM2* $^{-/-}$ mice with TRPM2 overexpression plasmids on E13.5. Then, on E16.5, we collected brain samples from mice that had been exposed to heat stress for 2 hours from E14.5 to E16.5. By staining with an anti-TUJ1 antibody, we found that *TRPM2*$^{-/-}$ mice not only exhibited an aberrant distribution of GFP-positive cells in three cortical layers but also showed a prominent increase in the proportion of GFP– and TUJ1–double positive cells compared with that in *TRPM2*$^{+/+}$ mice, which is reminiscent of *TRPM2* knockdown mice subjected to heat stress. Moreover, forced expression of TRPM2 in *TRPM2*$^{-/-}$ mice in hyperthermia could rescue the abnormalities evoked by the ablation of *TRPM2*, i.e., both the distribution and ratio of GFP$^+$ TUJ1$^+$ cells (Fig. 3, K to M). In addition, we also compared the distribution and ratio of GFP$^+$ TUJ1$^+$ cells between *TRPM2*$^{-/-}$ mice at room temperature and *TRPM2*$^{-/-}$ mice in hyperthermia groups. The results revealed that, upon exposure to hyperthermia, *TRPM2*$^{-/-}$ mice displayed a significant increase in the number of GFP-positive cells in the CP and the percentage of TUJ1$^+$GFP$^+$ cells (fig. S7, H to J). These findings demonstrate the vital role of TRPM2 during embryonic neurogenesis. In addition, the consistent phenotype of *TRPM2* knockout excludes the possibility of potential off-target effects of *TRPM2* shRNA in knockdown experiments. To investigate the effect of *TRPM2* deficiency on differentiating neurons in hyperthermia, we conducted an in vitro experiment using cultured primary neurons. The neurons were isolated from P0 hyperthermic *TRPM2*$^{+/+}$ and *TRPM2*$^{-/-}$ embryos and cultured in differentiation medium for 3 days. By staining with an antibody against TUJ1, we observed no obvious difference between the wild-type and *TRPM2* knockout groups in terms of neurite length or number of branches (fig. S8, K to M), suggesting that *TRPM2* deficiency induces no phenotype in neurons under heat stress. We also analyzed other stimuli, such as treatment with NaCl (fig. S8, N and Q), change in pH (fig. S8, O and R), and X radiation exposure (fig. S8, P and S), and subsequently found that TRPM2 was not activated by these stimuli. Overall, these findings indicate that well-regulated embryonic cortical development can be disturbed in hyperthermic conditions when *TRPM2* is deleted.

### TRPM2 modulates cortical neurogenesis by targeting SP5 during hyperthermia

To further detail how TRPM2 affects the developing brain in hyperthermia, we sequenced RNA (RNA-seq) to analyze transcriptome-wide changes that arise from the loss of *TRPM2*. Total RNA was acquired from the cortical tissue of E16 *TRPM2* knockout and wild-type mice with mothers that were housed at 38°C for 2 hours per day from E14.5 to E16.5. Sequencing was repeated twice for each sample to increase the reliability of the sequencing results. Gene Ontology (GO) analysis revealed that down-regulated genes were associated with cell proliferation and temperature stimuli, including the canonical Wnt signaling pathway, neuronal stem cell division, the detection of temperature stimuli involved in sensory perception, and the negative regulation of cell differentiation. The up-regulated genes were associated with neurogenesis, the regulation of neuronal development, and cell fate commitment (fig. S9A). These data jointly suggest a crucial role for the thermal sensor protein TRPM2 in cortical neurogenesis during hyperthermia. Next, we explored how the deletion of *TRPM2* affects neurogenesis at the molecular level during heat stress. Among the differentially expressed genes identified by genome analyses, we selected genes that changed consistently in both sequencing results and finally selected *SP5* as a downstream target (fig. S9B and Fig. 4A).

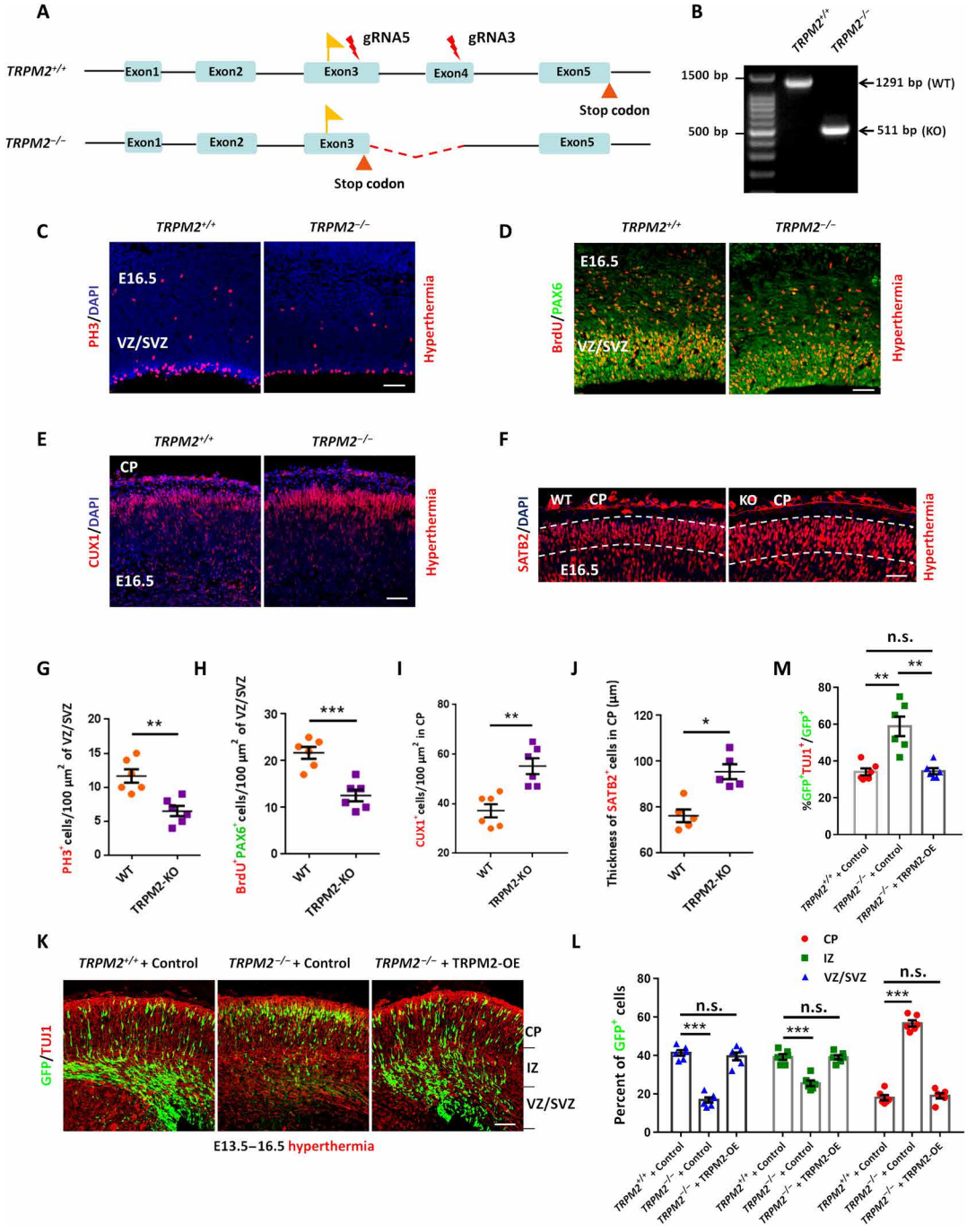


**Fig. 3. Deletion of *TRPM2* leads to aberrant embryonic neurodevelopment during heat stress.** (**A**) Schematic diagram of the generation of *TRPM2* knockout mice. (**B**) Genotyping of $TRPM2^{+/+}$ and $TRPM2^{-/-}$ mice. The results show that the PCR products of $TRPM2^{+/+}$ and $TRPM2^{-/-}$ were 1291 and 511 base pairs (bp), respectively. WT, wild type. (**C** and **G**) E16.5 brain slices from $TRPM2^{+/+}$ and $TRPM2^{-/-}$ mice were stained with DAPI and an antibody against PH3. Heat stress was applied from E14.5 to E16.5. The graph shows the number of PH3-positive cells per 100 $\mu m^2$ in the VZ/SVZ ($n = 6$). Scale bar, 20 μm. (**D** and **H**) $TRPM2^{+/+}$ and $TRPM2^{-/-}$ mice underwent 2 hours of BrdU pulse labeling and were sacrificed at E16.5. Brain slices were then stained with antibodies against BrdU and PAX6. The graph shows the number of $BrdU^+PAX6^+$ cells per 100 $\mu m^2$ in the VZ/SVZ ($n = 6$). Scale bar, 20 μm. (**E** and **I**) Coronal brain slices of E16.5 $TRPM2^{+/+}$ and $TRPM2^{-/-}$ mice were immunostained with an anti-CUX1 antibody. The number of $CUX1^+$ cells per 100 $\mu m^2$ of CP is shown ($n = 6$). Scale bar, 20 μm. (**F** and **J**) Representative images of E16.5 cortices showing SATB2-labeled cells. The graph shows the thickness of $SATB2^+$ cells in the upper layer of the CP ($n = 6$). Scale bar, 20 μm. (**K**) Deletion of *TRPM2* leads to abnormal cell distribution and neurogenesis defects during heat stress. Furthermore, these defects were rescued by the constitutive expression of TRPM2 in the developing brain. A GFP-expressing control vector or TRPM2 overexpression vector was microinjected and electroporated into E13.5 mouse brains. Heat stress was administered from E14.5 to E16.5 for 2 hours a day. The brains were collected on E16.5 and stained for TUJ1. (**L**) The population of GFP-positive cells in each region is displayed in the bar graph ($n = 6$ embryos from four different mothers). Scale bar, 50 μm. (**M**) The population of $TUJ1^+$ $GFP^+$ cells among $GFP^+$ cells is displayed in the bar graph ($n = 6$ embryos from four different mothers). Scale bar, 50 μm. The data are shown as means ± SEM; two-tailed Student's *t* tests; $^*P < 0.05$, $^{**}P < 0.01$, and $^{***}P < 0.001$ versus the indicated group.

To confirm the results of RNA-seq, we performed RT-PCR (fig. S9C) and Western blotting (fig. S9D) and observed that SP5 expression was significantly decreased in samples obtained from the cortex of *TRPM2* knockout mice that had experienced heat stress. SP5 is a transcription factor that is downstream of Wnt signaling (*17*, *19*), but the function of SP5 in cortical neurogenesis during hyperthermia has not yet been identified.

To investigate the function of SP5 in embryonic brain development, we first stained brain slices with a specific fluorescent antibody against SP5. The in vitro results showed that SP5 was expressed in the nuclei of primary mouse NSCs and was colocalized with progenitor markers, such as NESTIN and SOX2 (fig. S9G). Consistently, SP5 was expressed in vivo in NESTIN-positive NSCs in the VZ/SVZ of the E13.5 cortex (fig. S9H). Furthermore, shRNAs targeting SP5 were constructed, and they effectively silenced the expression of SP5 (fig. S10A). In addition, samples from heat stress–exposed mice in which the expression of SP5 was silenced showed an increased number of GFP-positive cells in the CP and a decreased number of GFP-positive cells located in the VZ/SVZ (Fig. 4, B and C). However, the redistribution of GFP-positive cells was not obvious in control mice from mothers that had been housed at room temperature (fig. S10, F and G). Immunostaining for KI67 also showed that fewer $GFP^+KI67^+$ cells were observed in the VZ/SVZ in SP5 knockdown mice that had been exposed to heat stress (fig. S10, B and C). In addition, we also found that the percentage of TUJ1-positive cells was obviously increased in neural progenitors that had been infected with an *SP5* shRNA–packaged lentivirus and had been exposed to hyperthermia (fig. S10, D and E). Overall, these data confirm that SP5 acts downstream of TRPM2 to modulate neurogenesis during heat stress.

### *TRPM2* deficiency decreases *SP5* levels via the repression of β-catenin enrichment on the SP5 promoter in hyperthermia

To further confirm and elucidate the specific mechanisms by which TRPM2 exerts its effect on NPC proliferation in hyperthermia, we monitored the relative mRNA levels of *SP5* and several molecular markers associated with proliferation. Transcription analysis revealed that β-*catenin* mRNA levels were reduced by 40% in *TRPM2* knockout NPCs from mice exposed to hyperthermia, while the levels of *REST*, *Hes5*, *SOX2*, *CyclinD1*, *Foxg1*, and *Olig2* were unchanged (fig. S9C). These findings suggest that β-catenin may work together with TRPM2 to regulate embryonic neurogenesis during heat stress. To compare the transcription results to translational outcome, we conducted Western blot analysis. Protein was obtained from E16 cortical tissue from *TRPM2* knockout and wild-type mice that were housed at 38°C for 2 hours per day from E14.5 to E16.5. Western blot analysis showed an obvious reduction in SP5 and β-catenin expression levels. We also found that the phosphorylation levels of β-catenin were augmented in *TRPM2* knockout mice exposed to hyperthermia. In addition, decreases in expression of the proliferative markers PH3 and PCNA (proliferating cell nuclear antigen) and an increase in the expression of the neuronal marker TUJ1 in *TRPM2* knockout mice clarified the role of TRPM2 in embryonic neurogenesis in hyperthermia (Fig. 4D). We obtained similar results in *TRPM2* knockdown or *TRPM2* overexpression primary NSCs exposed to 38°C (fig. S9, E and F). In *TRPM2* knockdown NPCs, immunostaining for total β-catenin verified that its expression was reduced during heat stress (fig. S10, H and I). We did not observe such an obvious change under room temperature conditions (fig. S6J). Intrigued by the altered phosphorylation levels of β-catenin in *TRPM2* knockout mice exposed to hyperthermia, we tested the activity of glycogen synthase kinase 3β (GSK3β), which is a serine/threonine kinase associated with β-catenin phosphorylation. On the basis of the fact that GSK3β activity requires the autophosphorylation of $Tyr^{216}$ (*30*), we evaluated protein levels and protein modifications. In *TRPM2* knockout mice exposed to hyperthermia, we observed an obvious increase in $Tyr^{216}$ phosphorylation, suggesting that TRPM2 may negatively regulate GSK3β activity (Fig. 4, E and F). The constitutive overexpression of TRPM2 during hyperthermia intensifies GSK3β activity (fig. S10K). In addition, Western blot analysis showed an increase in the expression of TRPM2, total β-catenin, and SP5 and a decrease in the phosphorylation of β-catenin (Fig. 4H). Together, these findings suggest that TRPM2 may modulate SP5 transcription by inhibiting the phosphorylation of β-catenin and activating β-catenin expression.

Intracellular calcium signaling plays key roles in neural development, including neuronal plasticity, neuronal survival, and neurogenesis (*31*). Studies have shown that intracellular calcium affects the β-catenin pathway (*32*). To further investigate the mechanisms by which TRPM2 plays a role in activating β-catenin expression, we measured the calcium ion concentration in NSCs using a confocal microscope and a calcium-sensitive dye. We observed that, when the cells were cultured at 38°C overnight, the intracellular calcium levels were significantly increased (Fig. 4, I and J). However, when cells were transfected with the *TRPM2*-sh1 plasmid with red fluorescent protein (RFP), intracellular calcium decreased (Fig. 4K), suggesting that TRPM2 modulates intracellular calcium. Calmodulin (CAM) is a target of calcium ions within the cell, and once bound to calcium ions, CAM is activated and serves as part of the calcium signal transduction pathway by modulating interactions with various target proteins (*33*). In our study, we found that CAM interacted with GSK3β (Fig. 4G), and Western blotting showed that phosphorylated β-catenin levels were reduced, while total β-catenin expression was slightly increased when CAM was overexpressed during heat stress (Fig. 4L). Therefore, these findings suggest that thermal stimuli activate TRPM2, which increases intracellular calcium. Calcium ions can then bind to CAM, thus inhibiting the levels of phosphorylated β-catenin and simultaneously activating the expression of β-catenin.

On the basis of these results, we suggest that β-catenin may enter the nucleus, bind to the SP5 promoter, and modulate the expression level of SP5 during heat stress. To test this hypothesis, we used a luciferase plasmid containing −2 kb of the SP5 promoter and measured luciferase activity (Fig. 5A). We also generated a vector that overexpressed β-catenin with a hemagglutinin (HA) tag and characterized its efficiency by Western blotting (fig. S10J). At 39°C, we observed more than twofold increase in luciferase activity in cells treated with the β-catenin vector compared with cells treated with the empty vector, demonstrating that β-catenin binds to the SP5 promoter to exert its function (Fig. 5A′). To further determine the specific binding site, we used a chromatin immunoprecipitation (ChIP) assay (Fig. 5B). At 39°C, in cells in which β-catenin was constitutively expressed, the binding of β-catenin −0.5 kb from the SP5 promoter increased, and binding decreased as the distance to the transcription start site increased (Fig. 5B′). These differences were not observed at 37°C (Fig. 5B″). In addition, we analyzed the promoters of other β-catenin target genes, such as *Axin2* and *CyclinD1*, in hyperthermia and observed that there was almost

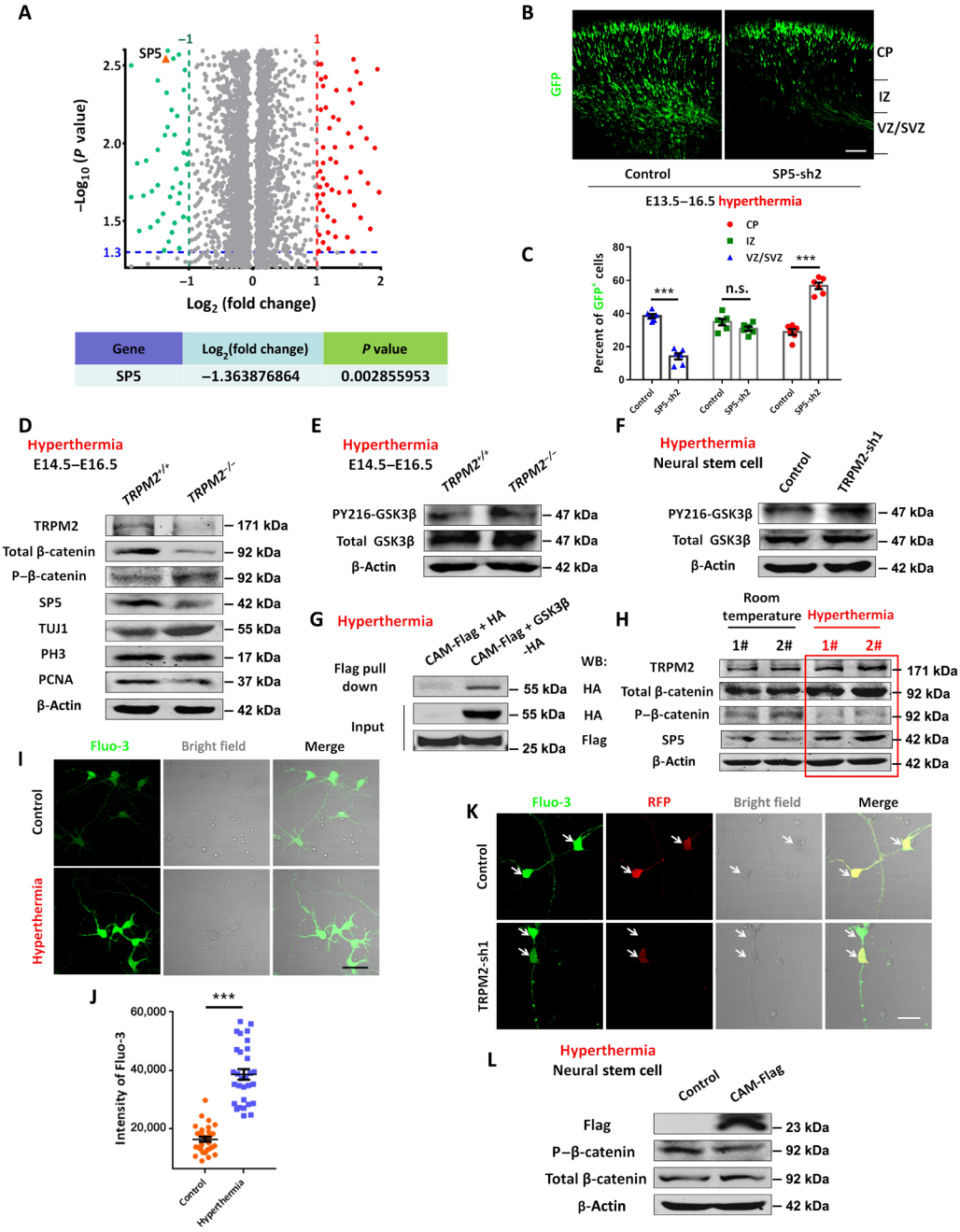


**Fig. 4. *TRPM2* modulates cortical neurogenesis by targeting *SP5* and regulating the phosphorylation and expression of β-catenin during heat stress.** (**A**) The volcano plot indicates differentially expressed genes. The red dots represent up-regulated genes, while the green dots represent down-regulated genes. *SP5* is one of the notably down-regulated genes. (**B** and **C**) *SP5* knockdown results in an abnormal cellular distribution during heat stress. The bar graph shows the population of $GFP^+$ cells in the CP, IZ, and VZ/SVZ ($n = 6$ embryos from four different mothers). Scale bar, 50 μm. (**D**) Western blot results showing the change in the expression of TRPM2, total β-catenin, phosphorylated β-catenin, SP5, TUJ1, PH3, and PCNA during heat stress in *TRPM2* knockout embryos. Heat stress was applied from E14.5 to E16.5 for 2 hours per day. β-Actin was used as the control ($n = 3$). (**E**) *TRPM2* knockout in vivo during hyperthermia increases GSK3β activity ($n = 3$). (**F**) The suppression of *TRPM2* in NSCs during heat stress intensifies GSK3β activity ($n = 3$). (**G**) Calmodulin (CAM) interacts with GSK3β in hyperthermia ($n = 3$). (**H**) Western blot analysis showing changes in the expression levels of TRPM2, total β-catenin, phosphorylated β-catenin, and SP5 between the brains of room temperature– and hyperthermia-exposed embryonic mice. β-Actin was used as the loading control ($n = 3$). (**I** and **J**) The intracellular calcium ion concentration increases upon exposure to 38°C. After neural stem cells were isolated from the E12.5 cortex cultured at 37°C or 38°C overnight, they were incubated for 30 min with Fluo-3, and the intracellular calcium fluorescence was quantified with a confocal LSM780 microscope. The graph shows the relative Fluo-3 intensity ($n = 30$). Scale bar, 15 μm. (**K**) Calcium concentration reduction is caused by *TRPM2* knockdown in hyperthermia. NSCs isolated from the E12.5 cortex were infected with a control or *TRPM2*-shRNA plasmid (red)–packaged lentivirus. After 6 hours, the cells were cultured at 38°C overnight; then, the calcium concentration was measured ($n = 3$). Scale bar, 5 μm. (**L**) Western blots showing the expression levels of Flag, total β-catenin, and phosphorylated β-catenin in primary NSCs with constitutively expressing CAM in hyperthermia conditions. β-Actin was used as a control ($n = 3$). The data are shown as means ± SEM; two-tailed Student's *t* tests; ***$P < 0.001$ versus the indicated group.

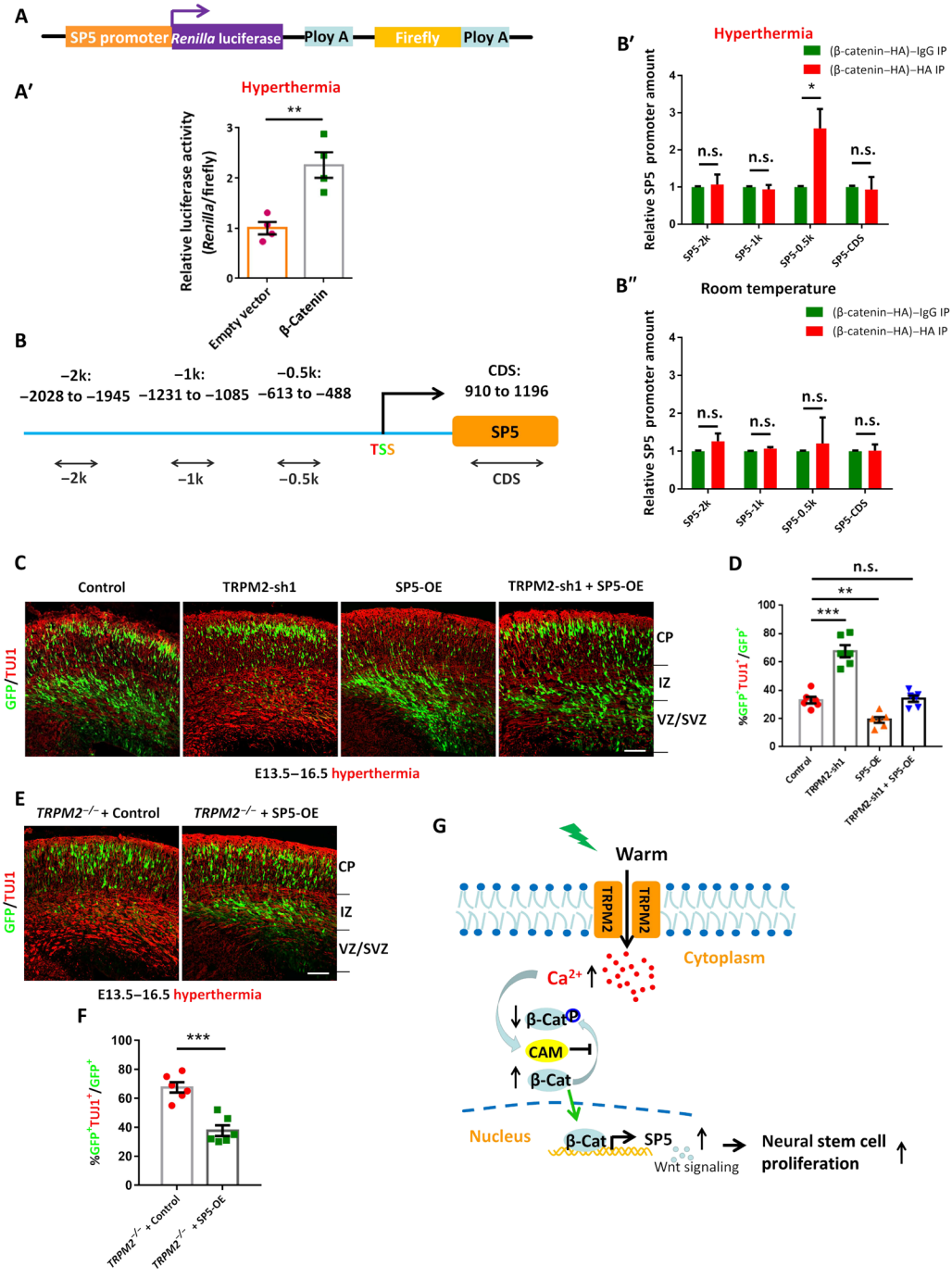


**Fig. 5. TRPM2 regulates cortical neurodevelopment through the enhancement of β-catenin enrichment on the SP5 promoter during heat stress.** (**A**) Flow chart of the luciferase assay in which the SP5 promoter was cloned into the psiCHECK-2 vector. (**A′**) 293FT cells were transfected with an empty vector or a β-catenin–expressing vector. Both groups were cotransfected with an SP5 promoter–containing psiCHECK-2 vector and cultured at 39°C. After 36 hours of transfection, the relative luciferase activity was quantified and is shown in the bar graph ($n = 4$). (**B**) Four pairs of primers were designed for −0.5, −1, and −2 kb from the SP5 transcription start sites and SP5 CDS for ChIP analysis. (**B′**) NPCs cultured in vitro at 39°C were infected with a β-catenin–HA–containing lentivirus and then pulled down using immunoglobulin G (IgG)– or HA-incubated magnetic beads. The relative amount of SP5 promoter was detected via ChIP and real-time PCR and is shown in the bar graph ($n = 3$). (**B″**) NPCs cultured in vitro at 37°C were infected with a β-catenin–HA–containing lentivirus and then pulled down with IgG- or HA-incubated magnetic beads. The relative amount of SP5 promoter was determined by ChIP and real-time PCR and is shown in the bar graph ($n = 3$). (**C** to **F**) SP5 overexpression rescues the cortical neurogenesis defects evoked by *TRPM2* knockdown (C and D) or knockout (E and F) in hyperthermia. After electroporation (E13.5) and heat stress (E14.5 to E16.5), E16.5 brain slices were stained with anti-TUJ1 antibody. The bar graphs show the percentage of $TUJ1^+GFP^+$ cells relative to the total number of $GFP^+$ cells ($n = 6$ embryos from four different mothers). Scale bars, 50 μm. (**G**) Working model of TRPM2 function in modulating cortical neurogenesis during heat stress. TRPM2 during heat stress increases calcium influx, which inhibits the phosphorylation of β-catenin and induces β-catenin enrichment on the SP5 promoter, thereby promoting NPC proliferation. The data are shown as means ± SEM; two-tailed Student's *t* tests; $^*P < 0.05$, $^{**}P < 0.01$, and $^{***}P < 0.001$ versus the indicated group.

no binding of β-catenin (fig. S10, L and M), suggesting specificity for SP5.

### Constitutive expression of SP5 partly rescues the *TRPM2* deficiency–induced phenotype in hyperthermia

To decipher the connection between TRPM2 and SP5 in neurogenesis during heat stress, we performed rescue experiments. We observed that the constitutive expression of SP5 increased the cell populations residing in the VZ/SVZ and ameliorated the irregularity of both the distribution and percentage of $GFP^+$ $TUJ1^+$ cells caused by *TRPM2* knockdown (Fig. 5, C and D) and knockout (Fig. 5, E and F) during heat stress in vivo. Therefore, these data demonstrate that SP5 acts downstream of TRPM2 to modulate early cortical development in hyperthermia. Together, our data supported the notion that, during heat stress, TRPM2 increases SP5 levels via the stabilization of β-catenin enrichment on the SP5 promoter, thus enhancing NPC proliferation (Fig. 5G).

## DISCUSSION

Cortical neurogenesis is a very sophisticated process that is strictly controlled by a great deal of signaling molecules. If any step of this process goes wrong, abnormal brain functions, and thus neurodevelopmental disorders, result (*34*). Temperature homeostasis is essential for embryo survival, and heat stress disturbs numerous aspects of fetal development and brain function (*35*). TRPM2, which has been recently identified as a heat activation protein, plays an important role in the heat response. TRPM2 is also a calcium-permeable channel in the plasma membrane, and a growing body of evidence has shown that calcium signaling heavily affects neural progenitor proliferation during embryonic neurogenesis (*10*, *36*). However, no details as to whether or how TRPM2 affects brain neural development under conditions of heat exist. Here, we used *TRPM2* shRNA and knockout mice to investigate the specific functions of TRPM2 in NPC proliferation and differentiation, cortical neuronal morphology, and the mechanisms guiding embryonic neurogenesis under hyperthermic conditions.

In our study, we first confirmed the thermal sensitivity of TRPM2 and then observed that TRPM2 is expressed in NSCs. When expressed during heat stress, TRPM2 augments NPCs in the E15.5 cerebral cortex, providing clues regarding its effect on neurogenesis during hyperthermia. Furthermore, we found that heat stress changes cellular distribution and facilitates NSC proliferation. Previous studies have shown that at room temperature, *TRPM2* loss of function leads to increased axonal growth to promote neuronal differentiation (*37*). Here, we demonstrated that TRPM2 can exert its function earlier, specifically at E13.5, and that during heat stress, the loss of *TRPM2* has a more powerful effect on facilitating cortical neurogenesis. However, at room temperature, the phenotype is not obvious. Our data indicate that *TRPM2* deficiency in hyperthermia results in a change in cell distribution and proliferation defects with a sharp drop in the NSC pool. We also found that the depletion of *TRPM2* during heat stress increases cell cycle exit and premature cell terminal mitosis, ultimately promoting neurons to a more differentiated state. Both proliferation defects and abnormalities in neuronal morphogenesis lead to severe brain illness, such as autism and schizophrenia (*38*, *39*). In addition, we were able to eliminate the influence of cell migration and apoptosis during hyperthermia by knocking out *TRPM2*. However, why the *TRPM2* knockdown phenotype observed during heat stress is more obvious than the phenotype observed under room temperature conditions still needs to be explored.

To investigate the mechanisms underlying the unique phenotype caused by the loss of *TRPM2* and hyperthermia, we searched for downstream targets using RNA-seq analysis and found that SP5 expression was decreased upon *TRPM2* knockout and hyperthermia. SP5 is a member of the SP1 family of transcription factors, but its function in embryonic brain development is still unclear.

Our research shows that SP5 is abundant in NPCs and that, under conditions of heat, *TRPM2* deficiency inhibits SP5 expression from E13.5 to E16.5. This leads to a decrease in the number of GFP-positive cells residing in the VZ/SVZ and results in the promotion of neuronal differentiation. To further decipher how TRPM2 enhances SP5 expression in hyperthermia, we analyzed some signaling molecules and found that total β-catenin expression was significantly downregulated, while the phosphorylation of β-catenin was obviously increased upon *TRPM2* deficiency and heat stress. β-Catenin, which functions in canonical Wnt signaling, is abundant in NSCs and contributes to the modulation of NSC expansion (*15*). However, specific mechanisms of the protein are not entirely clear. Previous studies have indicated that Wnt/β-catenin is associated with intracellular $Ca^+$ (*32*). Given that TRPM2 is a calcium-permeable channel, we investigated calcium ions during heat stress, and our data showed a decrease in intracellular $Ca^+$ levels upon *TRPM2* knockout. Moreover, the overexpression of CAM inhibited the phosphorylation of β-catenin and augmented the expression of β-catenin. Using a luciferase and ChIP assay, we also confirmed that β-catenin binds to the SP5 promoter during heat stress. Unexpectedly, our results indicated that the overexpression of SP5 ameliorates the defects evoked by *TRPM2* loss of function in hyperthermia. However, in the future, the current hyperthermia model needs to be further improved because in human, such as fever response, immune system component may take part in this model.

In summary, our findings uncovered a novel mechanism by which TRPM2, a thermo-sensor protein, governs embryonic neural development during heat stress. Furthermore, the neuronal morphology abnormalities in *TRPM2* knockout mice exposed to hyperthermia during embryonic development may provide novel insights into neurological disorders associated with heat stress, including maternal fever, and reveal new strategies for treatment. In terms of the mechanism, we found that when TRPM2 is activated by heat and intracellular calcium binds to CAM, the phosphorylation of β-catenin is inhibited. Accumulating β-catenin then binds to the SP5 promoter to ultimately enhance NPC proliferation.

## METHODS

### Animals

Pregnant ICR mice were obtained from Vital River Laboratories. All animal-related experiments were conducted in line with the Animal Care and Use Committee of Institute of Zoology, Chinese Academy of Sciences. *TRPM2* knockout mice used in our experiments were generated and kept in the Experiment Animal Center of Institute of Zoology, Chinese Academy of Sciences.

### Plasmid constructs

To construct shRNA-expressing plasmids, the oligonucleotides were inserted into the pSicoR-GFP (Addgene, 12093) or pSicoR-TOMATO

lentiviral vector. The sequences of shRNAs targeting TRPM2 were as follows: TRPM2-sh1, AACCTTAGCTCATGGATTC (*13*); TRPM2-sh2, GACCTTCTCATTTGGGCCGTT (Sigma). The sequences of SP5 shRNAs were as follows: SP5-sh1, GGATTCAAAGGATTTGCTTTC (*17*); SP5-sh2, CCCGTCGGACTTTGCACAG (Sigma). The full-length complementary DNAs (cDNAs) of mouse *TRPM2*, *SP5*, and *CAM* were obtained via PCR and cloned into the Flag-tagged pCDH (System Biosciences, CD511B-1) vector for lentivirus packaging.

### Cell culture

Human 293FT cells and mouse N2A cells were cultured in Dulbecco's modified Eagle's medium (DMEM) that contained 1% penicillin-streptomycin (PS) and 10% fetal bovine serum (FBS). Mouse cortical NPCs from E12.5 mouse cortex were maintained in proliferation medium, which contained 50% DMEM/F12 (Invitrogen), 50% neural basal medium (Invitrogen), epidermal growth factor (EGF) (10 ng/ml), basic fibroblast growth factor (bFGF) (10 ng/ml) (Invitrogen), 1% PS, and 2% B27 (without vitamin A).

### Lentivirus packaging and infection

The production of lentivirus was obtained by transfecting the core and packaging plasmids into 293FT cells using GenEscort I (Nanjing Wisegen Biotechnology). The virus was gathered at 24, 48, and 72 hours after changing the medium 6 hours after transfection. The primary NSCs for Western blot and immunofluorescence were seeded in 6- or 24-well plates, which were coated with laminin (Invitrogen) and poly-D-lysine (Sigma) (both 10 μg/ml) in advance. Twenty-four hours later, half of the medium was changed with proliferation medium without PS. Lentivirus was then added to each well and maintained for 8 hours. Meanwhile, to improve the infection efficiency, polybrene (2 μg/ml) was mixed into the medium. Forty-eight hours later, to induce a differentiation state, the medium was displaced with low-glucose DMEM (Gibco) supplemented with 1% FBS (Invitrogen), 1% PS, and 2% B27 (with vitamin A).

### In utero electroporation

IUE was performed as reported previously (*40*). In brief, pregnant ICR or C57 mice were deeply anesthetized with pentobarbital sodium (70 mg/kg). Subsequently, the recombinant knockdown or overexpression plasmids with a final concentration of 1500 ng/μl were mixed with an enhanced GFP plasmid at a ratio of 3:1. In addition, 0.02% Fast Green was included as a tracer. Then, the mixture was microinjected into the lateral ventricle of the embryonic mouse brains using glass capillaries. Five electric pulses of 40 V (950-ms interval; 50-ms duration) were generated using an electroporator (Manual BTX ECM 830) and platinum electrodes. After IUE, the brains of the embryos were collected at E16.5, E17.5, or P1 for further phenotype analysis.

### BrdU labeling

For neural progenitor proliferation analysis, BrdU (50 mg/kg) was injected 2 hours before brain harvesting at E16.5. For neuronal birth dating, BrdU (50 mg/kg) was administrated to pregnant mice at E14.5. For cell cycle exit analysis, BrdU (100 mg/kg) was administrated to pregnant mice 24 hours before brain collection at E15.5.

### Heat stress treatment

For heat stress experiments, mice were maintained in their cages, and the cages were put in a large temperature-controlled incubator set at 38° or 39°C for 2 hours each day for 2 or 3 days.

### Immunostaining

Brain slices or cells cultured in vitro were washed with phosphate-buffered saline (PBS) for 5 min, fixed in 4% paraformaldehyde for 20 min, and blocked in 5% bovine serum albumin (Sangon)/PBS containing 1% Triton X-100 (1% PBST) for 1 hour. Subsequently, the primary antibody was diluted with 1% PBST, added, and then incubated at 4°C overnight. The following day, the samples to be visualized were rinsed with PBS three times and incubated with secondary antibodies at room temperature for nearly 1.5 hours. The primary antibodies used for immunofluorescence are listed here: rabbit anti-TRPM2 (1:1000; Bethyl Laboratories), rabbit anti-TUJ1 (1:1000; Sigma), mouse anti-BrdU (1:1000; Millipore), rat anti-BrdU (1:1000; Abcam), rabbit anti-CUX1 (1:100; Santa Cruz Biotechnology), rabbit anti–cleaved caspase-3 (1:1000; Cell Signaling Technology), rabbit anti-PAX6 (1:1000; Millipore), mouse anti-MAP2 (1:1000; Millipore), mouse anti-NESTIN (1:1000; Millipore), rabbit anti-KI67 (1:1000; Abcam), mouse anti-SATB2 (1:300; Abcam), rabbit anti-SP5 (1:200; Bioss), rabbit anti-TBR2 (1:1000; Abcam), rat anti-CTIP2 (1:1000; Abcam), and mouse anti-SOX2 (1:1000; R&D Systems). Secondary antibodies applied were conjugates of Alexa Fluor Cy3, Cy5, or 488 (1:1000; Jackson ImmunoResearch). 4′,6-Diamidino-2-phenylindole (DAPI) (2 mg/ml; Sigma) was used for nuclear staining.

### Western blotting

Protein was extracted from brain cortical tissue of mouse or cultured cells by lysing with radioimmunoprecipitation assay buffer (Solarbio), with 10 mM phenylmethylsulfonyl fluoride and a protease inhibitor cocktail (Sigma, P8340). Samples were then ultrasonicated and centrifuged at approximately 12,000 rpm for 15 min at 4°C. Subsequently, the supernatants were gathered, and protein concentrations were determined using a BCA kit (Thermo Scientific). Next, similar amounts of protein samples were size-separated by 6 to 12% SDS–polyacrylamide gel electrophoresis gels and shifted onto nitrocellulose membranes (Whatman) making use of a semidry transfer system (Bio-Rad). We run multiple gels and normalized to a control. The primary antibodies applied in the Western blots are listed here: rabbit anti-TRPM2 (1:1000; Bethyl Laboratories and Novus Biologicals), rabbit anti–total β-catenin (1:1000; Cell Signaling Technology), rabbit anti–P–β-catenin (S33/S37/T41) (1:1000; Cell Signaling Technology), rabbit anti–non–P–β-catenin (S33/S37/T41) (1:1000; Cell Signaling Technology), rabbit anti-PCNA (1:500; Santa Cruz Biotechnology), rabbit anti-TUJ1 (1:1000; Bioward), rabbit anti-SP5 (1:500; Bioss), rabbit anti-PH3 (1:1000; Cell Signaling Technology), rabbit anti-TBR2 (1:1000; Abcam), and rabbit anti-Flag (1:1000; Sigma). Secondary antibodies were 800CW Donkey Anti-Mouse IgG (immunoglobulin G), 800CW Donkey Anti-Rabbit, 680LT Donkey Anti-Mouse IgG, and 680LT Donkey Anti-Rabbit IgG (LI-COR Biosciences). Odyssey v3.0 software was used to scan and quantify Western blot bands.

### Quantitative RT-PCR

Total RNA was obtained using TRIzol (Invitrogen, 15596) following the manufacturer's directions. Reverse transcription of mRNA to first-strand cDNA was achieved using the FastQuant RT Kit (TIANGEN). Quantitative RT-PCR was conducted using the SYBR Green PCR Kit (Takara) with an ABI PRISM 7500 sequence detector system (Applied Biosystems). All reactions were repeated in triplicate for each sample. The primer sequences used for RT-PCR are listed here: TRPM2, AAGGAACACAGACAATGCCTG (forward) and AGGATGGTCTTGTGGTTCGC; TRPM3, TACACCAAAGTCAGCTCCCTG

(forward) and GGCCTCTCGTGGAAAGTCAT (reverse); TRPM7, CCCAGCCAAGTTGCAAAAGT (forward) and CTACAGCTTTCTGCTTGCACC (reverse); TRPM8, GTCCTGTGACACCGACTCTG (forward) and CAGTGAGAATCCACGCACCT (reverse); TRPV1, CTCGGATGAATCTGAGCCCC (forward) and GACAACAGAGCTGACGGTGA (reverse); TRPV3, AGTGCTTATAGCAGCGGGTG (forward) and CGTGCAGGATGTTGTTTCCC (reverse); TRPV4, TCCTCTTCTCTTTCCCCGGT (forward) and GTGCCGTAGTCGAACAAGGA (reverse); ANO1, CGAGAAGTACTCGACGCTCC (forward) and TAGTCCACCTTCCGTTTGCC (reverse); TRPA1, TCTGCATATTGCCCTGCACA (forward) and ACTTTCATGCACTCGGGGAG (reverse); BDNF, TACCTGGATGCCGCAAACAT (forward) and GCCTTTGGATACCGGGACTT (reverse); PACAP, ATGACCATGTGTAGCGGAGC (forward) and CGCTGGATAGTAAAGGGCGT (reverse); β-catenin, ATCACTGAGCCTGCCATCTG (forward) and GTTGCCACGCCTTCATTC (reverse) (*39*); SP5, GGCAAGGTGTACGGCAAAAC (forward) and CATAGGTCCCGCGGATTCTC (reverse); REST, GTGCGAACTCACACAGGAGA (forward) and AAGAGGTTTAGGCCCGTTGT (reverse) (*41*); Hes5, CGCATCAACAGCAGCATAGAG (forward) and TGGAAGTGGTAAAGCAGCTTC (reverse); CyclinD1, GCCTACAGCCCTGTTACCTG (forward) and ATTTCATCCCTACCGCTGTG (reverse) (*42*); SOX2, GCACATGAACGGCTGGAGCAACG (forward) and TGCTGCGAGTAGGACATGCTGTAGG (reverse); Foxg1, GGCAAGGGCAACTACTGGAT (forward) and CGTGGTCCCGTTGTAACTCA (reverse); Olig2, GGTGTCTAGTCGCCCATCG (forward) and AGATGACTTGAAGCCACCGC (reverse); β-actin, GGTGGGAATGGGTCAGAAGG (forward) and AGGAAGAGGATGCGCCAGTG (reverse).

### ChIP–quantitative PCR

ChIP was performed as follows. To generate the cross-link, in vitro cultured cells were processed with 1% formaldehyde and maintained at room temperature for 10 min. Subsequently, 2.5 M glycine was then added to terminate the cross-link reaction. After washing three times with sterile PBS, the cells were gathered in lysis buffer. Next, the lysates were incubated with 15 μl of Dynabeads Protein G (Invitrogen), which was incubated at least 12 hours with 1 μg of specific antibody at 4°C before incubation. After washing three times with low- and high-salt buffer, the DNA-protein-antibody complex was incubated overnight at 65°C to open the covalent bond. Genomic DNA was then obtained using the TIANamp Genomic DNA Kit (TIANGEN Biotech) for subsequent real-time PCR analysis. The primer sequences applied for SP5 promoter are listed here: SP5-CDS, GGCAAGGTGTACGGCAAAAC (forward) and CATAGGTCCCGCGGATTCTC (reverse); SP5-0.5k, AGCTCGGTTGTGGGAGGAA (forward) and TCTTGACAAGCCGCTTGAAG (reverse); SP5-1k, ACCGCTGCCAGGTCGCT (forward) and AGGCAGGGTCAGTCGGC (reverse); SP5-2k, GCTGGGAACCGGTGGCT (forward) and TTGGGAGTATCCTCTTTGGC (reverse); CyclinD1-CDS, TCAAGACGGAGGAGACCTGT (forward) and TTCCGCATGGATGGCACAAT (reverse); CyclinD1-0.5k, CAGCCTCTTCCTCCACTTCC (forward) and AAGCCCTTCTGGAGTCAAGC (reverse); CyclinD1-1k, TCTACTTTAACAATGGTTTGCTGT (forward) and ACAGGGGAAGTCTTGAGAAGG (reverse); CyclinD1-2k, TCAGACATGGCCCTAAACCT (forward) and CATGACCAGTGTGACTCAAAGC (reverse); Axin2-CDS, CAAATGCAAAAGCCACCCGA (forward) and TGCATTCCGTTTTGGCAAGG (reverse); Axin2-0.5k, TACACACTCCCACCACCGA (forward) and ATCTCTGCTCACAGTTTCGGA (reverse); Axin2-1k, TGGAATGCAGTCTATCCCAGC (forward) and AGAAGCTGTGTGACCAGCCA (reverse); Axin2-2k, CCACCACAATCATCCTGGGT (forward) and TCAACTTTAAGGACTGAGGCCA (reverse).

### RNA-seq analyses

Global transcriptome analysis was conducted by Annoroad Company. Total RNA samples were first tested for quality and quantity using an Agilent 2100 bioanalyzer. After building the library, high-throughput sequencing was used with the Illumina HiSeq 2500 platform. Our RNA-Seq data were deposited in the Gene Expression Omnibus database with the accession number of GSE113954.

### *TRPM2* knockout mice construction

The CRISPR-Cas9 system was used to construct *TRPM2* knockout mice. During the process, two guide RNAs (gRNAs) (gRNA5, GCCAGTTCTTCTCCGGTCCAAGG; gRNA3, TATTGCTTCGTCGGAGATTGGGG) were used to cleave the whole genome sequence of TRPM2 to approximately 800 base pairs (bp). The genotyping primers designed for the *TRPM2* knockout mice were TRPM2-2717F GAAGGGAAACGGGTGGATGT and TRPM2-4007R GCAGGTCTCCTCAACCAGTC. The length of PCR product was 511 or 1291 bp for *TRPM2* knockout mice or wild-type mice, respectively.

### Cell apoptosis assay

Apoptotic cells were identified with immunostaining using an antibody targeting cleaved caspase-3.

### Luciferase assay

293FT cells ($4 \times 10^4$) were seeded into a 24-well plate and transfected with 0.5 μg of luciferase plasmid containing an SP5 promoter and empty vector or with 0.5 μg of luciferase plasmid containing an SP5 promoter and β-catenin overexpression vector, using GenEscort I (Nanjing Wisegen Biotechnology). Thirty-six hours after transfection, luciferase activity was measured using the Dual-Luciferase Assay System (Promega) and GloMax 96 Microplate Luminometer (Promega).

### Confocal imaging

All images were taken with a Zeiss LSM780 confocal microscope and analyzed with Photoshop CS6 (Adobe). ZEN 2010 was applied for image acquisition and processing. Brightness or expression quantity was measured using ImageJ when needed.

### Statistical analysis

All statistical analyses in this study were performed and plots were generated using GraphPad Prism7.0 software. Results are represented as means ± SEM. Two-tailed Student's *t* tests and one-way analysis of variance (ANOVA) were used for statistical comparisons. The differences were regarded as statistically significant with $*P < 0.05$, $**P < 0.01$, and $***P < 0.001$. n.s. means not significant.

## SUPPLEMENTARY MATERIALS

Supplementary material for this article is available at http://advances.sciencemag.org/cgi/content/full/6/1/eaay6350/DC1

Fig. S1. The expression pattern of TRPM2 and the detection of the efficiency of *TRPM2* knockdown and overexpression.

Fig. S2. Electroporation phenotypes under various conditions.

Fig. S3. *TRPM2* controls neural progenitor proliferation during heat stress.

Fig. S4. *TRPM2* loss of function promotes cell cycle exit and cortical neuron differentiation during heat stress.
Fig. S5. Deficiency of *TRPM2* during heat stress affects the development and morphology of neurons.
Fig. S6. Constitutive expression of TRPM2 rescues neurogenesis defects caused by *TRPM2* knockdown in hyperthermia.
Fig. S7. Ablation of *TRPM2* promotes neuronal differentiation and maturation and inhibits neural progenitor proliferation upon heat stress.
Fig. S8. Deletion of *TRPM2* changes neuron morphology and results in longer-term phenotypes in hyperthermia, but deficiency of *TRPM2* in differentiating neurons does not affect its development.
Fig. S9. *TRPM2* modulates cortical neurogenesis by targeting *SP5* in hyperthermia.
Fig. S10. *TRPM2* knockdown combined with heat exposure reduces SP5 expression by inhibiting β-catenin levels and the *SP5* knockdown phenotype.

View/request a protocol for this paper from *Bio-protocol*.

## REFERENCES AND NOTES


1. M. B. Woodworth, L. C. Greig, A. R. Kriegstein, J. D. Macklis, SnapShot: Cortical development. *Cell* **151**, 918–918.e1 (2012).
2. S. K. McConnell, Constructing the cerebral cortex: Neurogenesis and fate determination. *Neuron* **15**, 761–768 (1995).
3. D. Xu, F. Zhang, Y. Wang, Y. Sun, Z. Xu, Microcephaly-associated protein WDR62 regulates neurogenesis through JNK1 in the developing neocortex. *Cell Rep.* **6**, 104–116 (2014).
4. J. Dworkin, R. Losick, Linking nutritional status to gene activation and development. *Genes Dev.* **15**, 1051–1054 (2001).
5. C. Li, D. Xu, Q. Ye, S. Hong, Y. Jiang, X. Liu, N. Zhang, L. Shi, C. F. Qin, Z. Xu, Zika virus disrupts neural progenitor development and leads to microcephaly in mice. *Cell Stem Cell* **19**, 672 (2016).
6. L. Pei, H. Zhu, R. Ye, J. Wu, J. Liu, A. Ren, Z. Li, X. Zheng, Interaction between the SLC19A1 gene and maternal first trimester fever on offspring neural tube defects. *Birth Defects Res. A Clin. Mol. Teratol.* **103**, 3–11 (2015).
7. Q. Y. Shi, J. B. Zhang, Y. Q. Mi, Y. Song, J. Ma, Y. L. Zhang, Congenital heart defects and maternal fever: Systematic review and meta-analysis. *J. Perinatol.* **34**, 677–682 (2014).
8. M. J. Caterina, M. A. Schumacher, M. Tominaga, T. A. Rosen, J. D. Levine, D. Julius, The capsaicin receptor: A heat-activated ion channel in the pain pathway. *Nature* **389**, 816–824 (1997).
9. J. Vriens, G. Owsianik, T. Hofmann, S. E. Philipp, J. Stab, X. Chen, M. Benoit, F. Xue, A. Janssens, S. Kerselaers, J. Oberwinkler, R. Vennekens, T. Gudermann, B. Nilius, T. Voets, TRPM3 is a nociceptor channel involved in the detection of noxious heat. *Neuron* **70**, 482–494 (2011).
10. C. H. Tan, P. A. McNaughton, The TRPM2 ion channel is required for sensitivity to warmth. *Nature* **536**, 460–463 (2016).
11. J. C. Belrose, M. F. Jackson, TRPM2: A candidate therapeutic target for treating neurological diseases. *Acta Pharmacol. Sin.* **39**, 722–732 (2018).
12. K. Togashi, Y. Hara, T. Tominaga, T. Higashi, Y. Konishi, Y. Mori, M. Tominaga, TRPM2 activation by cyclic ADP-ribose at body temperature is involved in insulin secretion. *EMBO J.* **25**, 1804–1815 (2006).
13. L. Sun, H. Y. Yau, W. Y. Wong, R. A. Li, Y. Huang, X. Yao, Role of TRPM2 in $H_2O_2$-induced cell apoptosis in endothelial cells. *PLOS ONE* **7**, e43186 (2012).
14. S. Huang, E. Turlova, F. Li, M. H. Bao, V. Szeto, R. Wong, A. Abussaud, H. Wang, S. Zhu, X. Gao, Y. Mori, Z. P. Feng, H. S. Sun, Transient receptor potential melastatin 2 channels (TRPM2) mediate neonatal hypoxic-ischemic brain injury in mice. *Exp. Neurol.* **296**, 32–40 (2017).
15. H. Clevers, K. M. Loh, R. Nusse, Stem cell signaling. An integral program for tissue renewal and regeneration: Wnt signaling and stem cell control. *Science* **346**, 1248012 (2014).
16. S. M. Harrison, D. Houzelstein, S. L. Dunwoodie, R. S. Beddington, Sp5, a new member of the Sp1 family, is dynamically expressed during development and genetically interacts with Brachyury. *Dev. Biol.* **227**, 358–372 (2000).
17. S. Ye, D. Zhang, F. Cheng, D. Wilson, J. Mackay, K. He, Q. Ban, F. Lv, S. Huang, D. Liu, Q. L. Ying, Wnt/β-catenin and LIF-Stat3 signaling pathways converge on Sp5 to promote mouse embryonic stem cell self-renewal. *J. Cell Sci.* **129**, 269–276 (2016).
18. D. S. Park, J. H. Seo, M. Hong, W. Bang, J. K. Han, S. C. Choi, Role of Sp5 as an essential early regulator of neural crest specification in xenopus. *Dev. Dyn.* **242**, 1382–1394 (2013).
19. G. Weidinger, C. J. Thorpe, K. Wuennenberg-Stapleton, J. Ngai, R. T. Moon, The Sp1-related transcription factors sp5 and sp5-like act downstream of Wnt/β-catenin signaling in mesoderm and neuroectoderm patterning. *Curr. Biol.* **15**, 489–500 (2005).
20. R. Sacco, E. Cacci, G. Novarino, Neural stem cells in neuropsychiatric disorders. *Curr. Opin. Neurobiol.* **48**, 131–138 (2018).
21. S. M. Perez, D. D. Aguilar, J. L. Neary, M. A. Carless, A. Giuffrida, D. J. Lodge, Schizophrenia-like phenotype inherited by the F2 generation of a gestational disruption model of schizophrenia. *Neuropsychopharmacology* **41**, 477–486 (2016).
22. J. Vriens, T. Voets, Heat sensing involves a TRiPlet of ion channels. *Br. J. Pharmacol.* **176**, 3893–3898 (2019).
23. C. L. Tan, E. K. Cooke, D. E. Leib, Y. C. Lin, G. E. Daly, C. A. Zimmerman, Z. A. Knight, Warm-sensitive neurons that control body temperature. *Cell* **167**, 47–59.e15 (2016).
24. U. Lendahl, L. B. Zimmerman, R. D. McKay, CNS stem cells express a new class of intermediate filament protein. *Cell* **60**, 585–595 (1990).
25. Q. F. Wu, L. Yang, S. Li, Q. Wang, X. B. Yuan, X. Gao, L. Bao, X. Zhang, Fibroblast growth factor 13 is a microtubule-stabilizing protein regulating neuronal polarization and migration. *Cell* **149**, 1549–1564 (2012).
26. K. K. Singh, X. Ge, Y. Mao, L. Drane, K. Meletis, B. A. Samuels, L. H. Tsai, Dixdc1 is a critical regulator of DISC1 and embryonic cortical development. *Neuron* **67**, 33–48 (2010).
27. J. I. Heng, L. Nguyen, D. S. Castro, C. Zimmer, H. Wildner, O. Armant, D. Skowronska-Krawczyk, F. Bedogni, J. M. Matter, R. Hevner, F. Guillemot, Neurogenin 2 controls cortical neuron migration through regulation of Rnd2. *Nature* **455**, 114–118 (2008).
28. A. Duque, P. Rakic, Different effects of bromodeoxyuridine and [$^3$H]thymidine incorporation into DNA on cell proliferation, position, and fate. *J. Neurosci.* **31**, 15205–15217 (2011).
29. B. Lehner, B. Sandner, J. Marschallinger, C. Lehner, T. Furtner, S. Couillard-Despres, F. J. Rivera, G. Brockhoff, H. C. Bauer, N. Weidner, L. Aigner, The dark side of BrdU in neural stem cell biology: Detrimental effects on cell cycle, differentiation and survival. *Cell Tissue Res.* **345**, 313–328 (2011).
30. P. A. Lochhead, R. Kinstrie, G. Sibbet, T. Rawjee, N. Morrice, V. Cleghon, A chaperone-dependent GSK3β transitional intermediate mediates activation-loop autophosphorylation. *Mol. Cell* **24**, 627–633 (2006).
31. A. B. Toth, A. K. Shum, M. Prakriya, Regulation of neurogenesis by calcium signaling. *Cell Calcium* **59**, 124–134 (2016).
32. C. Thrasivoulou, M. Millar, A. Ahmed, Activation of intracellular calcium by multiple Wnt ligands and translocation of β-catenin into the nucleus: A convergent model Wnt/Ca2+ and Wnt/β. *J. Biol. Chem.* **288**, 35651–35659 (2013).
33. D. Chin, A. R. Means, Calmodulin: A prototypical calcium sensor. *Trends Cell Biol.* **10**, 322–328 (2000).
34. C. Ernst, Proliferation and differentiation deficits are a major convergence point for neurodevelopmental disorders. *Trends Neurosci.* **39**, 290–299 (2016).
35. H. Asakura, Fetal and neonatal thermoregulation. *J. Nippon Med. Sch.* **71**, 360–370 (2004).
36. P. Uhlen, N. Fritz, E. Smedler, S. Malmersjo, S. Kanatani, Calcium signaling in neocortical development. *Dev. Neurobiol.* **75**, 360–368 (2015).
37. Y. Jang, M. H. Lee, J. Lee, J. Jung, S. H. Lee, D. J. Yang, B. W. Kim, H. Son, B. Lee, S. Chang, Y. Mori, U. Oh, TRPM2 mediates the lysophosphatidic acid-induced neurite retraction in the developing brain. *Pflugers Arch.* **466**, 1987–1998 (2014).
38. Y. Watanabe, K. Khodosevich, H. Monyer, Dendrite development regulated by the schizophrenia-associated gene FEZ1 involves the ubiquitin proteasome system. *Cell Rep.* **7**, 552–564 (2014).
39. Y. Mao, X. Ge, C. L. Frank, J. M. Madison, A. N. Koehler, M. K. Doud, C. Tassa, E. M. Berry, T. Soda, K. K. Singh, T. Biechele, T. L. Petryshen, R. T. Moon, S. J. Haggarty, L.-H. Tsai, Disrupted in schizophrenia 1 regulates neuronal progenitor proliferation via modulation of GSK3β/β-catenin signaling. *Cell* **136**, 1017–1031 (2009).
40. T. Saito, In vivo electroporation in the embryonic mouse central nervous system. *Nat. Protoc.* **1**, 1552–1558 (2006).
41. C. A. Mao, W. W. Tsai, J. H. Cho, P. Pan, M. C. Barton, W. H. Klein, Neuronal transcriptional repressor REST suppresses an Atoh7-independent program for initiating retinal ganglion cell development. *Dev. Biol.* **349**, 90–99 (2011).
42. W. Xia, Y. Liu, J. Jiao, GRM7 regulates embryonic neurogenesis via CREB and YAP. *Stem Cell Rep.* **4**, 795–810 (2015).



**Acknowledgments**
**Funding:** This work was supported by grants obtained from the National Science Fund for Distinguished Young Scholars (81825006), CAS Strategic Priority Research Program (XDA16010301), National Key R&D Program of China (2019YFA0110300 and 2018YFA0108402), National Science Foundation of China (31730033 and 31621004), and K. C. Wong Education Foundation. **Author contributions:** Y.L. performed the experiments, analyzed data, and wrote the manuscript. J.J. conceived and supervised this project. **Competing interests:** The authors declare that they have no competing interests. **Data and materials availability:** All data needed to evaluate the conclusions in the paper are present in the paper and/or the Supplementary Materials. Additional data related to this paper may be requested from the authors.

Submitted 5 July 2019
Accepted 4 November 2019
Published 1 January 2020
10.1126/sciadv.aay6350

**Citation:** Y. Li, J. Jiao, Deficiency of TRPM2 leads to embryonic neurogenesis defects in hyperthermia. *Sci. Adv.* **6**, eaay6350 (2020).